

# $\gamma$ -Fe<sub>2</sub>O<sub>3</sub>/ZnO composite particles prepared by a two step chemical soft method

S. López-Romero and F. Morales Leal

*Instituto de Investigaciones en Materiales, Universidad Nacional Autónoma de México,*

*Apartado Postal 70-360, México D.F., 04510, México,*

*e-mails: sebas@servidor.unam.mx; fnleal@servidor.unam.mx*

Recibido el 3 de febrero de 2011; aceptado el 8 de abril de 2011

Composite iron oxide-Zinc oxide ( $\gamma$ -Fe<sub>2</sub>O<sub>3</sub>/ZnO) was synthesized by two step method: in the first one step  $\gamma$ -Fe<sub>2</sub>O<sub>3</sub> particles were obtained by a cetyltrimethylammonium hydroxide (CTAOH) assisted hydrothermal method at low temperature (60°C). In the second step, the  $\gamma$ -Fe<sub>2</sub>O<sub>3</sub> particles were included in the ZnO particles synthesis, which were obtained by a hexamethylenetetramine (HMTA) assisted hydrothermal method at low temperature (90°C). SEM study of the samples revealed that the  $\gamma$ -Fe<sub>2</sub>O<sub>3</sub>/ZnO composites present a compact morphology. The  $\gamma$ -Fe<sub>2</sub>O<sub>3</sub> and ZnO phases were identified by XRD, energy dispersive X-ray analysis (EDX) and analysis of the IR spectrum. The composite exhibit the characteristic emissions of ZnO under UV radiation and ferromagnetic behavior of  $\gamma$ -Fe<sub>2</sub>O<sub>3</sub> under an external magnetic field.

**Keywords:** Iron oxides; zinc oxides; hydrothermal method; composites.

En este trabajo el compuesto formado entre el óxido de hierro y el óxido de zinc ( $\gamma$ -Fe<sub>2</sub>O<sub>3</sub>/ZnO) fue sintetizado por el método sol-gel en dos pasos: en el primer paso partículas del óxido de hierro  $\gamma$ -Fe<sub>2</sub>O<sub>3</sub> fueron obtenidas por el método hidrotérmico asistido con hidróxido de cetiltrimetilamonio (CTAOH) a baja temperatura (60°C). En el segundo paso, las partículas del óxido  $\gamma$ -Fe<sub>2</sub>O<sub>3</sub> fueron incluidas en la síntesis de las partículas de ZnO las cuales fueron obtenidas por el método hidrotérmico asistido con hexametilentetramina HMTA) a una temperatura de 90°C. El análisis SEM de las muestra reveló que las partículas del compuesto  $\gamma$ -Fe<sub>2</sub>O<sub>3</sub>/ZnO presentan una morfología redonda compacta. Las fases  $\gamma$ -Fe<sub>2</sub>O<sub>3</sub> y ZnO fueron identificadas por XRD, análisis de rayos x con energía dispersiva (EDX), y análisis de espectro IR. El compuesto exhibe emisión característica del ZnO bajo radiación UV y comportamiento ferromagnético del  $\gamma$ -Fe<sub>2</sub>O<sub>3</sub> bajo un campo magnético.

**Descriptores:** Óxido de hierro; óxido de zinc; método hidrotérmico; materiales compuestos.

PACS: 81.05Mh

## 1. Introduction

The synthesis of composite particles consisting of magnetic cores and luminescent cells such as  $\gamma$ -Fe<sub>2</sub>O<sub>3</sub>/ZnO has gained acceptance in few years due to its magnetic, photoluminescence and catalytic properties [1]. Also, as active element in gas sensors [2]. This type of composite particles has biological and biomedical potential applications such as detection of cancer cells, bacteria and viruses, and magnetic separation [3]. Recently Ruipeng Fu *et al.* [4] prepared  $\gamma$ -Fe<sub>2</sub>O<sub>3</sub>/ZnO composite particles via a simple solution method, and investigated its morphology; indicating that the  $\gamma$ -Fe<sub>2</sub>O<sub>3</sub>/ZnO composite particles are of typical sphere-like morphology with diameter in the range of 300-400 nm. Also, the  $\gamma$ -Fe<sub>2</sub>O<sub>3</sub>/ZnO composites exhibit magnetic response to an external magnetic field and efficient characteristic emissions of ZnO under UV excitation. Dong Kee Yi *et al.* [5], by a two step synthesis obtained silica-coated nanocomposites of  $\gamma$ -Fe<sub>2</sub>O<sub>3</sub> magnetic nanoparticles (MPs) and CdSe photoluminescent quantum dots (QDs), its analysis showed that the presence of CdSe increased the effective magnetic anisotropy of the  $\gamma$ -Fe<sub>2</sub>O<sub>3</sub> containing particles, indicating that the QDs were closely connected to MPs, concluding that the SiO<sub>2</sub>/MPs-QDs nanocomposite particles preserved the magnetic properties of  $\gamma$ -Fe<sub>2</sub>O<sub>3</sub> and optical properties of CdSe QDs. Hongwei Gu [1] reported on a one-pot chemical synthesis method for generating heterodimers of nanoparticles by taking advantage of lattice Mismatch and selective an-

nealing at a relatively low temperature. They deposited amorphous CdS on the surface of FePt nanoparticles to form a metastable core-shell structure, in which the CdS transformed into a crystalline state upon heating. Moreover, the core shell structures which have sizes less than 10 nm, also exhibit both superparamagnetism and fluorescence.

In this work, we report on a two-step surfactant assisted hydrothermal method to synthesize  $\gamma$ -Fe<sub>2</sub>O<sub>3</sub>/ZnO composite particles. In the first step  $\gamma$ -Fe<sub>2</sub>O<sub>3</sub> nanoparticles were synthesized by a sol-gel method using ferric nitrate [Fe(NO<sub>3</sub>)<sub>3</sub>] as source material and cetyltrimethylammonium hydroxide (CTAOH) as surfactant and catalyst. In the second step zinc nitrate [Zn(NO<sub>3</sub>)<sub>2</sub>.6H<sub>2</sub>O] and hexamethylenetetramine, also called methenamina were taken as starting materials.

## 2. Experimental details

### 2.1. Materials

All chemicals (Sigma Aldrich) used in this study were of analytical reagent grade and used without further purification.

### 2.2. Preparation of $\gamma$ -Fe<sub>2</sub>O<sub>3</sub> nanoparticles

The process to obtain a colloidal solution to synthesize the  $\gamma$ -Fe<sub>2</sub>O<sub>3</sub> nanoparticles is based on the sol-gel method [6]. Briefly: ferric nitrate (Fe(NO<sub>3</sub>)<sub>3</sub>) and cetyltrimethylammo-

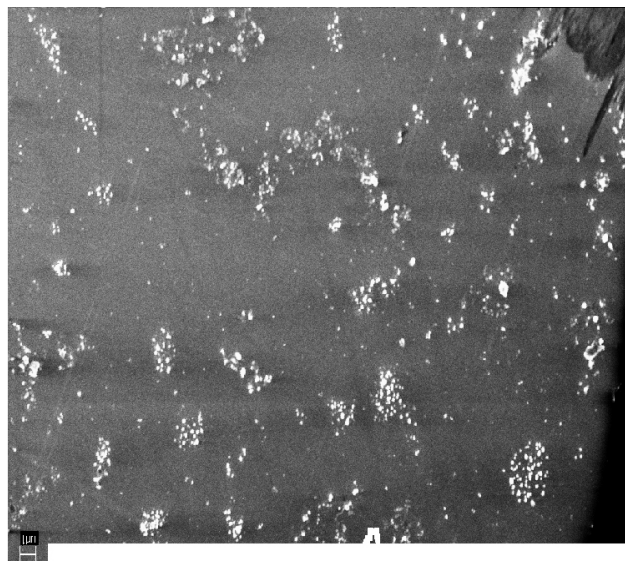


FIGURE 1. Scanning electron microscopy image of the seed magnetic  $\gamma$ -Fe<sub>2</sub>O<sub>3</sub> particles.

nioum hydroxide (CTAOH) were taken as starting materials. Initially 0.01 M of ferric nitrate was dissolved in ethyl alcohol and magnetically stirred at 60°C for 1 h. Then, cetyltrimethylammonium hydroxide was mixed into solution with a molar ratio of Fe<sup>3+</sup>/CTAOH of 1/1.6 and later refluxed at 60°C for 2 h. After few minutes the solution became dark-red, which indicated the  $\gamma$ -Fe<sub>2</sub>O<sub>3</sub> nanoparticles formation. Finally, after refluxing for 2 h the solution was cooled to room temperature, and a black-red precipitate was obtained upon adding alcohol and centrifuging.

### 2.3. Preparation of $\gamma$ -Fe<sub>2</sub>O<sub>3</sub>/ZnO composites particles

The synthesis method to obtain the  $\gamma$ -Fe<sub>2</sub>O<sub>3</sub>/ZnO composite particles is as follow: Zinc nitrate (Zn(NO<sub>3</sub>)<sub>2</sub>·6H<sub>2</sub>O) was taken as the source material and hexamethylenetetramine ((CH<sub>3</sub>)<sub>6</sub>N<sub>4</sub>) as the surfactant and catalyst. The precursor was prepared by dissolving 3.0 g of Zinc nitrate and 8.0 g of methanamina in deionized water under vigorous stirring at 30°C for 1h to form a 0.01 M equimolar solution. Then, the  $\gamma$ -Fe<sub>2</sub>O<sub>3</sub> nanoparticles prepared in the before step, were deposited into the solution and heated at 90°C for 10 h. It was observed that a pink powder precipitated at the flask bottom, indicating the  $\gamma$ -Fe<sub>2</sub>O<sub>3</sub>/ZnO composites particles formation.

## 3. Characterization

The x-ray diffraction patterns of  $\gamma$ -Fe<sub>2</sub>O<sub>3</sub>/ZnO composites were obtained with an x-ray diffractometer (SIEMENS D 500) using the CuK <sub>$\alpha$</sub>  ( $\lambda$ =1.5406 Å) radiation, with a scanning speed of 1° per min, 35 kV and 30 mA, the scanning in  $2\theta$  was from 2 to 70°. Morphology of the composite samples and analysis X-ray EDX were obtained using a JEM600-Lv scanning electron microscopy. IR spectra of the  $\gamma$ -Fe<sub>2</sub>O<sub>3</sub>/ZnO composite particles in KBr pellets were

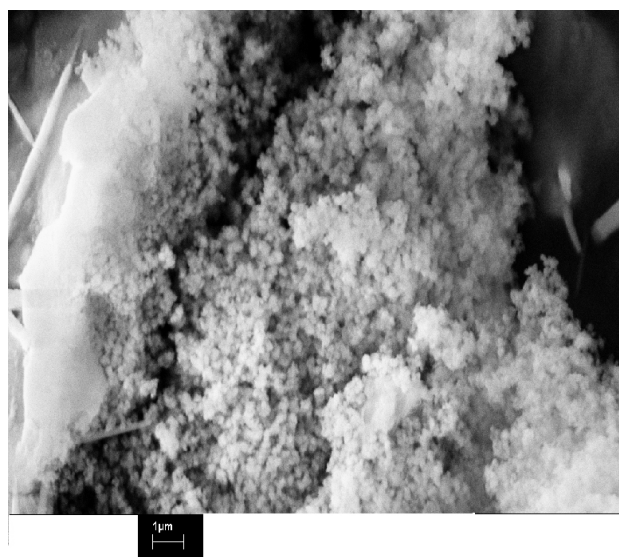


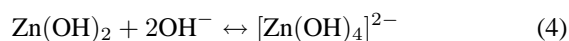
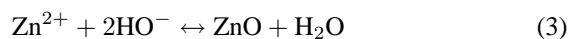
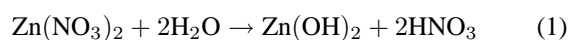
FIGURE 2. SEM image of  $\gamma$ -Fe<sub>2</sub>O<sub>3</sub>/ZnO composite particles.

recorded in the range of 4000-500 cm<sup>-1</sup> on an American Nicolet AVANTAR 380 FT-IR spectrometer. The photoluminescence spectrum was obtained using a fluorescence spectrometer (Hitachi.H-4600). Magnetization (M) measurements were performed with a SQUID based magnetometer (Quantum Design). The temperature (T) range of measurements was between room temperature and 2 K, and the range of applied magnetic field (H) in these experiments was between  $\pm$  10 kOe. M(T) measurements were performed in the zero field cooling (ZFC) and field cooling (FC) mode.

## 4. Results and discussion

Figure 1 is a SEM image of the magnetic  $\gamma$ -Fe<sub>2</sub>O<sub>3</sub> nanoparticles prepared by the first step of the method. The nanoparticles are non uniform monodispersed and have a grain size in the range of 100-200 nm, and can be considered as sphere-like particles. Figure 2 is a SEM image of as-synthesized  $\gamma$ -Fe<sub>2</sub>O<sub>3</sub>/ZnO composite particles; they present a compact morphology and are bigger than the  $\gamma$ -Fe<sub>2</sub>O<sub>3</sub> seed particles. The grain size of the composite particles is in the range of 400-600 nm.

Consistent with the reaction mechanisms proposed in hydrothermal syntheses [7], which has established that the growth unit are the anions [Zn(OH)<sub>4</sub>]<sup>2-</sup>, the following chemical reactions are proposed:



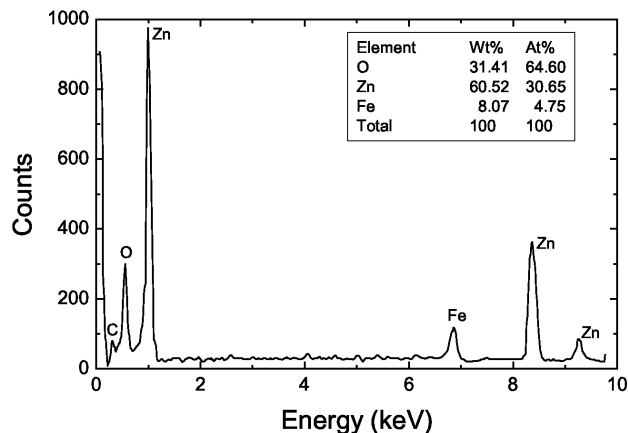
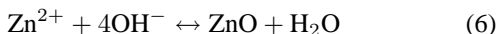
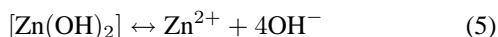


FIGURE 3. Composition and EDX of the  $\gamma$ -Fe<sub>2</sub>O<sub>3</sub>/ZnO composite.



In reaction (1) Zn<sup>2+</sup> ions are first combined with OH<sup>-</sup> radicals in the aqueous solution to form a Zn(OH)<sub>2</sub> colloid via the reaction Zn<sup>2+</sup> + 2OH<sup>-</sup> → Zn(OH)<sub>2</sub>. Later, in the hydrothermal process a portion of the Zn(OH)<sub>2</sub> is separated into Zn<sup>2+</sup> ions and OH<sup>-</sup> radicals according to reaction (2). Then, ZnO nuclei are formed according to the reaction (3), when the concentration of Zn<sup>2+</sup> ions and OH<sup>-</sup> radicals reaches the supersaturation degree of ZnO. Finally, the growth units of [Zn(OH)<sub>4</sub>]<sup>2-</sup> radicals are replicated by means of reaction (4). Continuing thus with the dissolution-nucleation cycle according to reactions (5) and (6), respectively.

Figure 3 shows the composition and the image of EDX of the  $\gamma$ -Fe<sub>2</sub>O<sub>3</sub>/ZnO composite. Zn, Fe and O elements belonged  $\gamma$ -Fe<sub>2</sub>O<sub>3</sub>/ZnO composite.

The Fe to Zn ratio initial in wt% was of 0.8 and the same ratio taken from the EDX measurement was of 0.15.

Figure 4 shows the XRD patterns of the  $\gamma$ -Fe<sub>2</sub>O<sub>3</sub>/ZnO composites obtained at room temperature. The diffraction peaks of ZnO are marked by diamonds, corresponding to the hexagonal phase with lattice constants;  $a = 3.25 \text{ \AA}$  and  $c = 5.21 \text{ \AA}$  (JCPD file No 36-1451). The lattice parameters obtained for this samples are  $a = 3.24880 \text{ \AA}$  and  $c = 5.20540 \text{ \AA}$ . The peaks marked by dots were indexed to the cubic phase of  $\gamma$ -Fe<sub>2</sub>O<sub>3</sub> with  $a = 4.822 \text{ \AA}$  (JCPDS file No 39-1346). The lattice parameter obtained in this case is  $a = 4.682 \text{ \AA}$ , concluding that the x-ray pattern showed that in the composite  $\gamma$ -Fe<sub>2</sub>O<sub>3</sub>/ZnO particles each compound conserve its crystalline structures.

Figure 5 shows the FT IR spectrum of the  $\gamma$ -Fe<sub>2</sub>O<sub>3</sub>/ZnO composite. The broad band centered at 3433 cm<sup>-1</sup> can be assigned to the stretching vibration of OH<sup>-</sup>. The peaks at 1747 and 1702 cm<sup>-1</sup> are due at CO<sup>-</sup> groups. The peak at 1643 cm<sup>-1</sup> is assigned to COOFe groups. The absorptions at 1389, 1149 and 1064 cm<sup>-1</sup> can be ascribed to the COO-

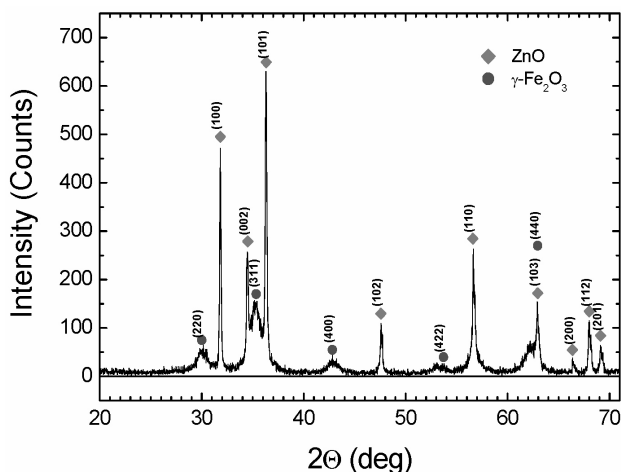


FIGURE 4. XRD pattern of  $\gamma$ -Fe<sub>2</sub>O<sub>3</sub>/ZnO composite particles. The diffraction peaks of ZnO are indicated by diamonds and the diffractions peaks of  $\gamma$ -Fe<sub>2</sub>O<sub>3</sub> are indicated by dots.

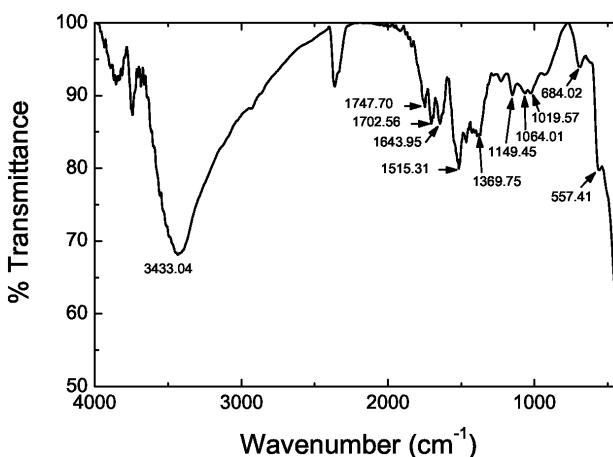


FIGURE 5. FT IR spectrum of  $\gamma$ -Fe<sub>2</sub>O<sub>3</sub>/ZnO composite particles.

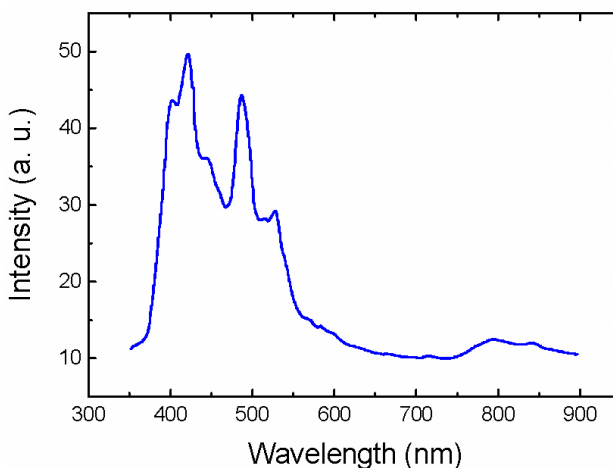


FIGURE 6. Spectrum of photoluminescence of  $\gamma$ -Fe<sub>2</sub>O<sub>3</sub>/ZnO composite particles under 358 nm excitation.

groups. The peak at 684 cm<sup>-1</sup> is a characteristic absorption of  $\gamma$ -Fe<sub>2</sub>O<sub>3</sub>. The peak at 554 cm<sup>-1</sup> is a characteristic absorp-

tion of ZnO. All these IR spectrum data are in consistence with the reported values [8-11].

Figure 6 shows the room temperature photoluminescence spectrum of the  $\gamma$ -Fe<sub>2</sub>O<sub>3</sub>/ZnO composite particles, obtained with a laser radiation of 358 nm. It is well known that the emission spectra of a ZnO particle consist of two emission bands: the first is an exciton emission band in the UV region with a maximum in  $\sim$  380 nm, this band is caused by the radiative annihilation of excitons, and the second, an intense band in the green region of the visible spectrum with a maximum in between 500 and 530 nm due to the radiative recombination of an electron from a level in the conduction band and a deeply trapped hole in the bulk ( $V''_0$ ) of an ZnO particle [12,13]. In Fig. 6 it is observed that the exciton emission occurs near ultraviolet (380-400 nm) and the visible emission occur in the green light (480 nm) regions. In addition to, the figure 6 shows that the intensity of the emission visible is less than the intensity of exciton emission. This is due according to Van Dijken [13] to an effect of particle size in which to point out that as the size of the ZnO particles increases the intensity of visible emission decreases and the intensity of exciton emission increases. In our case, from Fig. 2 the  $\gamma$ -Fe<sub>2</sub>O<sub>3</sub>/ZnO particles size ( $\sim$  300nm) is bigger than Dijken particles decreasing thus the intensity of visible emission respect to that of exciton emission. The occurrence of the exciton and visible peaks in photoluminescence spectrum confirm the presence of ZnO in the  $\gamma$ -Fe<sub>2</sub>O<sub>3</sub>/ZnO composite.

The temperature dependence of magnetic behavior  $M(T)$  of the  $\gamma$ -Fe<sub>2</sub>O<sub>3</sub>/ZnO composite shows a difference between the ZFC and FC measurements as is shown in Fig. 7. The ZFC and FC curves show an irreversible temperature region that finish about a maximum in the ZFC curve. This maximum is about 12 K and it is independent of magnetic field as shown by the curves measured a magnetic field of 10 Oe and 1 kOe. Similar  $M(T)$  behavior has been observed in  $\gamma$ -Fe<sub>2</sub>O<sub>3</sub> nanoparticles with size around 6.4 nm [14], however,

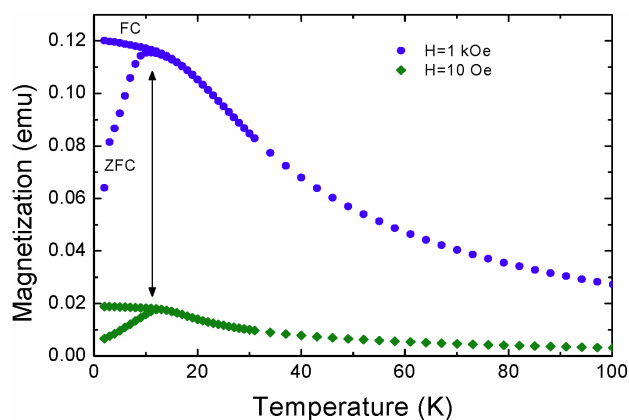


FIGURE 7. Magnetization as a function of temperature of the  $\gamma$ -Fe<sub>2</sub>O<sub>3</sub>/ZnO composite. Measurements correspond to the same sample under magnetic field of 10 Oe and 1 kOe, in the ZFC and FC mode. The arrows indicate the maximum in the ZFC curve that occurs at  $T=12$  K.

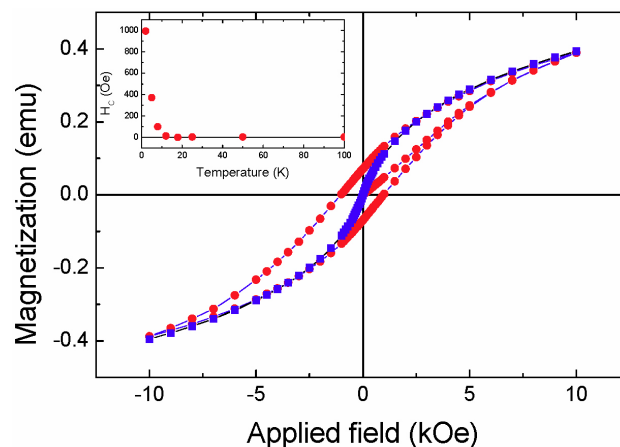


FIGURE 8. Magnetization as a function of applied magnetic field of a sample of  $\gamma$ -Fe<sub>2</sub>O<sub>3</sub>/ZnO composite, the curves were measured at 2 K (circles) and 12 K (squares). Note that the curve measured at 12 K does not show hysteresis. The inset shows the coercive field as a function of temperature.

the temperature where the maximum occurs in the ZFC curve depends from applied magnetic field. This temperature has been associated with the blocking temperature and change from 101 K, when the applied field was a 200 Oe, to 68 K under a field of 50 Oe [15].

Magnetization as a function of magnetic field at low temperatures shows hysteretic behavior. Figure 8 shows  $M(H)$  cycles obtained at 5 and 12 K. The hysteretic behavior disappears when the temperature is increased, it occurs at about 12 K. From this temperature and above  $M(H)$  shows a superparamagnetic behavior, as can be observed in the curve measured at 12 K (Fig. 8). Measurements of  $M(H)$  at temperatures 12 K and above do not show hysteresis. This behavior is in agreement with the temperature at which the  $M(T)$  curve shows difference between the ZFC and FC measurements. The inset in Fig. 8 shows the temperature behavior of the coercive field ( $H_C$ ) from 2 K until 100 K. The coercive field observed at 5 K is about 300 Oe, higher than 20 Oe reported for nanoparticles of 6.8 nm [15] and lower than 1 kOe reported for nanoparticles of 8.5 nm [14]. It is noted that  $H_C(T)$  decreases almost exponentially. This behavior is in disagreement to the  $H_C \propto T^{1/2}$  behavior observed in  $\gamma$ -Fe<sub>2</sub>O<sub>3</sub> nanoparticles with diameter distribution from 3 to 5 nm [16,17]. As mentioned above, the  $\gamma$ -Fe<sub>2</sub>O<sub>3</sub> nanoparticles size is between 100-200 nm, it could be interesting to know if the exponential behavior of  $H_C(T)$  is related to the particles size.

## 5. Conclusions

In this work were synthesized compact  $\gamma$ -Fe<sub>2</sub>O<sub>3</sub>/ZnO composite particles by a two step assisted-hydrothermal method. From studies made by SEM microscopy, the morphology of the composite particles resulted to be compact with a grain size in the range of 400-600 nm. The phases and purity of the  $\gamma$ -Fe<sub>2</sub>O<sub>3</sub>/ZnO composite particles were investigated by

XRD, EDX and IR analysis and revealed that the  $\gamma$ -Fe<sub>2</sub>O<sub>3</sub> and the ZnO nanoparticles conserved its phases respective. From photoluminescence and magnetic behavior M(T) studios of the  $\gamma$ -Fe<sub>2</sub>O<sub>3</sub>/ZnO composite particles can be conclude that the ZnO and  $\gamma$ -Fe<sub>2</sub>O<sub>3</sub> particles preserved the unique optic property of the first and magnetic property of the second.

## Acknowledgements

The author gratefully acknowledge useful contribution with L. Baños and Adriana Tejada for his support in carrying out x-ray study, Omar Novelo for their support in electron microscopy characterization and Miguel A. Canseco for his support in carrying out IR study.

- 
1. Hongwei Gu *et al*, *J. Am. Chem. Soc.* **126** (2004) 5664.
  2. Teixeira *et al*, *J. Bra. Chem. Soc.* **11** (2000) 27
  3. Deseng Wang *et al.*, *Nano Lett.* **3** (2004) 409.
  4. Ruipeng Fu *et al.*, *Mater. Lett.* **62** (2008) 4066.
  5. Don Kee Yi, *et al.*, *J. Am. Chem. Soc.* **127** (2005) 499.
  6. Chin-Hsien Hung and Wha-Tzong Wang, *Mater. Chem. Phys.* **82** (2003) 705.
  7. Yongshen Zang *et al.*, *Appl. Sur. Sci.* **242** (2005) 212.
  8. Xiang Yang Kong and Zhong Lin Wang, *Nano Lett.* **3** (2003) 1625.
  9. Sihui Zhang *et al*, *Coll. Interface Sci* **308** (2007) 265.
  10. M. Andres-Verges and C.J. Cerna, *J. Mater Sci. Let.* **7** (1988) 970.
  11. Zhijon Jing, *J. Mater. Lett.* **60** (2006) 2217.
  12. Svetozar Music *et al*, *J. Alloys Comp.* **448** (20008) 277.
  13. S. Monticone *et al*, *J. Phys. Chem. B.* **102** (1998) 2854.
  14. A. Van Dijken *et al*, *J. Luminescence* **87-89** (2000) 454.
  15. P. Duita *et al*, *Phys. Rev. B* **70** (2004) 174428.
  16. K. Jhon, *et al*, *J. Appl. Phys.* **73** (1993) 5109.
  17. Jong-Ryul Jeong, *et al*, *Phys. Status Solidi B* **241** (2004) 1593.